Efficient upscaling of hydraulic conductivity in heterogeneous alluvial aquifers

Jan H. Fleckenstein · Graham E. Fogg

Abstract An efficient method to upscale hydraulic conductivity (K) from detailed three-dimensional geostatistical models of hydrofacies heterogeneity to a coarser model grid is presented. Geologic heterogeneity of an alluvial fan system was characterized using transition-probability-based geostatistical simulations of hydrofacies distributions. For comparison of different hydrofacies architecture, two alternative models with different hydrofacies structures and geometries and a multi-Gaussian model, all with the same mean and variance in K, were created. Upscaling was performed on five realizations of each of the geostatistical models using the arithmetic and harmonic means of the K-values within vertical grid columns. The effects of upscaling on model domain equivalent K were investigated by means of steady-state flow simulations. A logarithmic increase in model domain equivalent K with increasing upscaling, was found for all fields. The shape of that upscaling function depended on the structure and geometry of the hydrofacies bodies. For different realizations of one geostatistical model, however, the upscaling function was the same. From the upscaling function a factor could be calculated to correct the upscaled K-fields for the local effects of upscaling.

Résumé Une méthode efficace pour upscale la conductivité hydraulique (K) à partir de modèles géostatistiques 3D détaillés de l'hétérogénéité d'hydrofaciès vers un maillage de modèle plus grossier est présentée. L'hétérogénéité géologique d'un système de cône alluvial a été caractérisée en utilisant des simulations géostatistiques basées sur une probabilité d'évolution des distributions d'hydrofaciès. Pour comparer plusieurs compositions d'hydrofaciès deux modèles alternatifs avec des structures d'hydrofaciès et des géométries différentes et un modèle Gaussien multiple, tous avec la même moyenne et variance de K, ont été créés. L'upscaling a été réalisé sur cinq mises en œuvre de chacun des modèles géostatistiques en utilisant les moyennes arithmétiques et harmoniques des valeurs K au sein de colonnes verticales du maillage. Les effets de l'upscaling de l'équivalent K dans le domaine du modèle ont été étudiés au moyen de simulations en écoulement permanent. Un accroissement logarithmique de l'équivalent K dans le domaine du modèle avec un upscaling croissant, a été trouvé pour tous les domaines. La forme de cette fonction d'upscaling dépendait de la structure et de la géométrie des ensembles d'hydrofaciès. Pour différentes mises en œuvre d'un modèle géostatistique, toutefois, la fonction d'upscaling était la même. A partir de la fonction d'upscaling un facteur peut être calculé pour corriger les domaines de K upscaled des effets locaux de l'upscaling.

Resumen Se presenta un método eficiente para el sobre-escalado de la conductividad hidráulica (K) a partir de modelos geoestadísticos tridimensionales de heterogeneidades de hidrofacies a modelos con grillas de mayor escala. La heterogeneidad geológica de un abanico aluvial se caracterizó usando probabilidad de transición basada en simulaciones de la distribución de las hidrofacies. Para la comparación de la arquitectura de las distintas hidrofacies, se crearon dos modelos alternativos con diferentes estructuras y geometrías de las hidrofacies y un modelo multi-gaussiano, con la misma media y varianza de K. El sobre-escalado se logró con cinco realizaciones de cada modelo geoestadístico usando las medias aritmética y armónica de los valores de K en cada columna vertical de la grilla. Los efectos del sobre-escalado se investigaron con simulaciones del flujo en estado estacionario. Se halló que un incremento en el sobre-escalado produce un incremento logarítmico en el dominio del modelo con K equivalente. La forma de la función de sobre-escalado depende de la estructura y geometría de los cuerpos de hidrofacies. Sin embargo, para diferentes realizaciones de un dado modelo geoestadístico, la función de sobre-escalado fue la misma. Esa función de sobre-escalado permite calcular un factor que corrige los campos de K sobre-escalados por efectos locales del sobre-escalado.

Received: 26 August 2007 / Accepted: 14 April 2008
Published online: 3 June 2008

J. H. Fleckenstein (✉)
Department of Hydrology,
University of Bayreuth,
Universitätsstrasse 30, 95447 Bayreuth, Germany
e-mail: jan.fleckenstein@uni-bayreuth.de
Tel.: +49-921-552147
Fax: +49-921-552366

G. E. Fogg
Department of Land, Air and Water Resources and
Department of Geology,
University of California, Davis,
1 Shields Avenue, Davis, CA 95616 USA

 DOI 10.1007/s10040-008-0312-3

Keywords Upscaling · Hydraulic properties · Heterogeneity · Geostatistics · Numerical modeling

Introduction

Heterogeneities are naturally present in most geologic materials at different spatial scales, from the pore scale (<cm) to the scale of hydrofacies (tens to several hundred meters) (de Marsily et al. 2005). Hydrofacies-scale heterogeneities in aquifers have been shown to significantly affect groundwater flow (Ababou et al. 1989; Webb and Anderson 1996; Eaton 2006), transport (LaBolle and Fogg 2001; Scheibe and Yabusaki 1998) and groundwater–surface-water interactions (Fleckenstein et al. 2006). With advances in computing power, it has become common practice to include representations of geologic heterogeneity even in large groundwater flow models (Tompson et al. 1999; Weissmann et al. 2002; Fleckenstein et al. 2006). Geostatistical techniques are readily available to create relatively realistic subsurface distributions of hydrofacies (Robin et al. 1993; Ritzi et al. 1994; Webb 1995; Koltermann and Gorelick 1996; Carle et al. 1998; Deutsch and Journel 1998; de Marsily et al. 1998; Zappa et al. 2006) often with several million grid cells. Solving flow models for such large grids can still pose numerical challenges. Therefore, upscaling techniques, which can reduce the number of grid cells from a detailed description of geologic heterogeneity to a tractable flow model, are necessary (Journel 1996; Wen et al. 2003; Noetinger et al. 2005). It is not only important to reduce grid size, but also to capture the specific hydrofacies architecture (e.g. connectivity), which is of paramount importance for flow and transport (Fogg et al. 2000; Zinn and Harvey 2003; Knudby and Carrera 2005; Sanchez-Vila et al. 2006). A simple form of upscaling for flow based on averaging of hydrofacies hydraulic conductivities (K) is presented here. It allows the incorporation of detailed small-scale representations of geologic heterogeneity into a larger scale groundwater-flow model, while maintaining the most important structural features of the geology. An alluvial fan system in California (Cosumnes River) was chosen as a test site. The architecture of the alluvial hydrofacies was characterized using geostatistical indicator simulations based on transition probabilities and Markov chains (Carle and Fogg 1996, 1997; Carle 1999). To assess the effects of upscaling on model block equivalent K, numerical experiments were conducted for different geostatistical models representing different hydrofacies structures and for five realizations of each geostatistical model.

Upscaling of hydraulic conductivity

Upscaling methods for K have been the focus of much research. It is beyond the scope of this paper to give a full account of this large body of work. Instead, some basic concepts that will put the presented methodology into a larger context will be outlined. For more detailed discussions of the topic the reader is referred to extensive reviews of upscaling methods presented by Wen and Gomez-Hernandez (1996); Renard and de Marsily (1997); Cushman et al. (2002); Neuman and Di Frederico (2003) and Sanchez-Vila et al. (2006).

The general purpose of upscaling K is to find a single value of K for an entire flow domain or a larger block of an aquifer that, for arbitrary (effective K) or given boundary conditions (apparent or equivalent K), yields the same flow through the homogeneous upscaled domain or block as through the original heterogeneous one (Renard and de Marsily 1997). Effective K is defined in the probability space as the conductivity that relates the expected value of specific discharge to the expected value of the head gradient in a quasi-infinite stationary domain (Renard and de Marsily 1997; Dagan 2001; Sanchez-Vila et al. 2006). As it is uniform in space and independent of the boundary conditions, it represents a characteristic property of the aquifer or porous medium (Sanchez-Vila et al. 2006). In real aquifers, however, the conditions for an effective K to emerge are practically never met. Therefore, the terms pseudoeffective K (Sanchez-Vila et al. 2006) or apparent K are used (Dagan 2001), if K varies in space due to boundary conditions or non-stationarity of the aquifer material. In physical space, the term equivalent K (Rernard and de Marsily 1997; Dagan 2001) or block-averaged K (Wen and Gomez-Hernandez 1996; Sanchez-Vila et al. 2006) is used for K-values obtained by averaging over larger aquifer blocks. This paper is concerned with averaging K in physical space. The terms "upscaled K" and "equivalent K" are therefore used synonymously (see also Sanchez-Vila et al. 2006).

Renard and de Marsily (1997) distinguished deterministic, stochastic, and heuristic upscaling methods. Deterministic methods assume full knowledge of the underlying heterogeneity model, whereas stochastic methods account for uncertainties by taking a probabilistic view. Heuristic methods try to derive rules to calculate plausible values of equivalent K. Within each group of methods, analytical and numerical solutions can be used and methods can be local or non-local. In local methods, equivalent K only depends on the properties within an upscaled block, whereas non-local methods also account for effects of external blocks (Renard and de Marsily 1997). Deterministic methods are either based on some constitutive theory (e.g. percolation theory, theory of effective media, renormalization, etc.; e.g. Renard et al. 2000) or on analytical or numerical solutions to the governing flow equations (e.g. Chen et al. 2003; Wen et al. 2003, 2006). Constitutive theories and analytical solutions to the flow equations often require simplifying assumptions such as simple geology (e.g. binary media, layered systems) or simple flow (e.g. steady state, two-dimensional flow). Although numerical solutions to the governing flow equations allow the most general treatment of upscaling problems and are least restrictive in the representation of geologic structures and boundary and flow conditions, they can be very computationally expensive for large, complex systems (Chen et al. 2003).

 DOI 10.1007/s10040-008-0312-3

Stochastic methods usually describe effective parameters as random functions that can be described by their moments (Renard and de Marsily 1997). Analytical expressions for effective K can be derived under specific assumptions about (1) the statistical properties of the K-field such as log-normality (e.g. Tartakovsky and Neumann 1998; Jankovic et al. 2003), binary K distribution (e.g. Fiori et al. 2003, Pozdniakov and Tsang 2004), bimodal K distributions (e.g. Rubin 1995), and (2) specific flow and boundary conditions, e.g. two-dimensional flow (e.g. Fiori et al. 2003), radial flow (e.g. Desbarats 1994, Indelman 2003) or transient flow with slowly varying hydraulic gradients (Tartakovsky and Neumann 1998). Tartakovsky and Guadagnini (2004) have proposed an approach for non-stationary, binary composites under one and two-dimensional steady-state flow.

Heuristic methods use simple averages to compute equivalent K. The value of equivalent K for a block of material with a given K distribution lies between an upper and lower bound, which in the most general case is given by the Wiener bounds (harmonic mean = lower bound and arithmetic mean = upper bound). A common way to describe the range of equivalent K between the Wiener bounds is the power average (Journel et al. 1986),

$$K_{eff} = \langle K^p \rangle^{1/p} = \left(\frac{1}{V} \int_V K(x)^p dV \right)^{1/p} \quad (1)$$

where V is the block volume and p the power exponent or p-norm ranging from –1 to 1. For p=–1, Eq. 1 describes the harmonic mean (lower bound) and for p=1, the arithmetic mean (upper bound). In the limit of p approaching zero, Eq. 1 yields the geometric mean.

Heuristic methods are simple and fast, but local, meaning they do not account for effects of neighboring blocks and macroscopic boundary conditions on equivalent K. As Renard and de Marsily (1997) point out, the different methods should rather be seen as complementary and not as antagonistic; and, depending on the problem, different methods might be applicable. Stochastic methods can account for uncertainties but use restrictive assumptions in their analytical developments (Renard and de Marsily 1997), deterministic methods based on numerical flow solutions are generally applicable but computationally expensive (especially if they are non-local, e.g. Chen et al. 2003) and heuristic methods are fast but local.

Objectives

In hydrogeological practice complex, three-dimensional hydrofacies models with multiple facies and multimodal, discontinuous K distributions are increasingly used for flow and transport simulations. Existing methods to upscale such subsurface models are limited to computationally expensive, numerical approaches. The main objective of this study was to develop and test a new computationally less demanding procedure to efficiently upscale hydraulic K from detailed three-dimensional geostatistical hydrofacies models with more than two categories, to coarser-scale groundwater flow models. The starting point was an existing three-dimensional hydrofacies model of an alluvial fan system with four hydrofacies, which was to be upscaled for flow simulations. In that sense, the focus of this work was more on practical application than on theoretical development. In the choice of an appropriate method, three requirements had to be met: (1) the procedure should preserve important, local structural elements such as hydrofacies connectivity of the original three-dimensional hydrofacies model (connectivity is loosely defined here as a concept that describes the degree to which high K hydrofacies form continuous paths between individual grid cells and across the entire model domain); (2) it should be efficient and fast so that upscaling could be performed on numerous realizations of a geostatistical model and (3) it should be able to accurately reproduce net flow through the model domain. These requirements ruled out the available, more theoretically driven upscaling methods, the deterministic, numerical ones due to their speed and the deterministic, analytical and stochastic ones due to their restrictive assumptions. Therefore, a local heuristic approach with a subsequent empirical correction of the obtained equivalent K values for non-local effects based on numerical experiments was chosen. In that context, three questions were addressed: (1) How does the proposed upscaling affect the distribution of K in the domain?; (2) Can consistent relationships (functions) between the degree of upscaling and equivalent K (K_{eq}) be found for different realizations of one specific geostatistical model?; (3) How does the structure of hydrofacies arrangements in the model affect the upscaling relationship? Effects of the proposed upscaling on transport parameters such as effective dispersion were not addressed in this study.

Methods

Geostatistical simulation of aquifer heterogeneity

Three-dimensional geostatistical models of geologic heterogeneity were generated for a stream-dominated alluvial fan aquifer in California (Cosumnes River) by sequential indicator simulations based on transition probabilities and Markov Chains using the software TPROGS (Carle 1999; Carle and Fogg 1996, 1997). In the models, four distinct hydrofacies, gravel and coarse sand, sand, (channel deposits) muddy sand (near channel deposits) and mud (silt and/or clay-undifferentiated floodplain deposits) were distinguished (Weissmann et al. 1999). Cell dimensions in depositional strike-, dip- and vertical-directions were 100, 200 and 0.5 m respectively. For a detailed description of model construction see Fleckenstein (2004) and Fleckenstein et al. (2006). From five realizations (R1–R5) of the original geostatistical model, a 60 m thick, 20×10 km subdomain consisting of 102×100×120 cells was used for the upscaling experiments (Fig. 1). The K-values in Table 1 were assigned to the four

 DOI 10.1007/s10040-008-0312-3

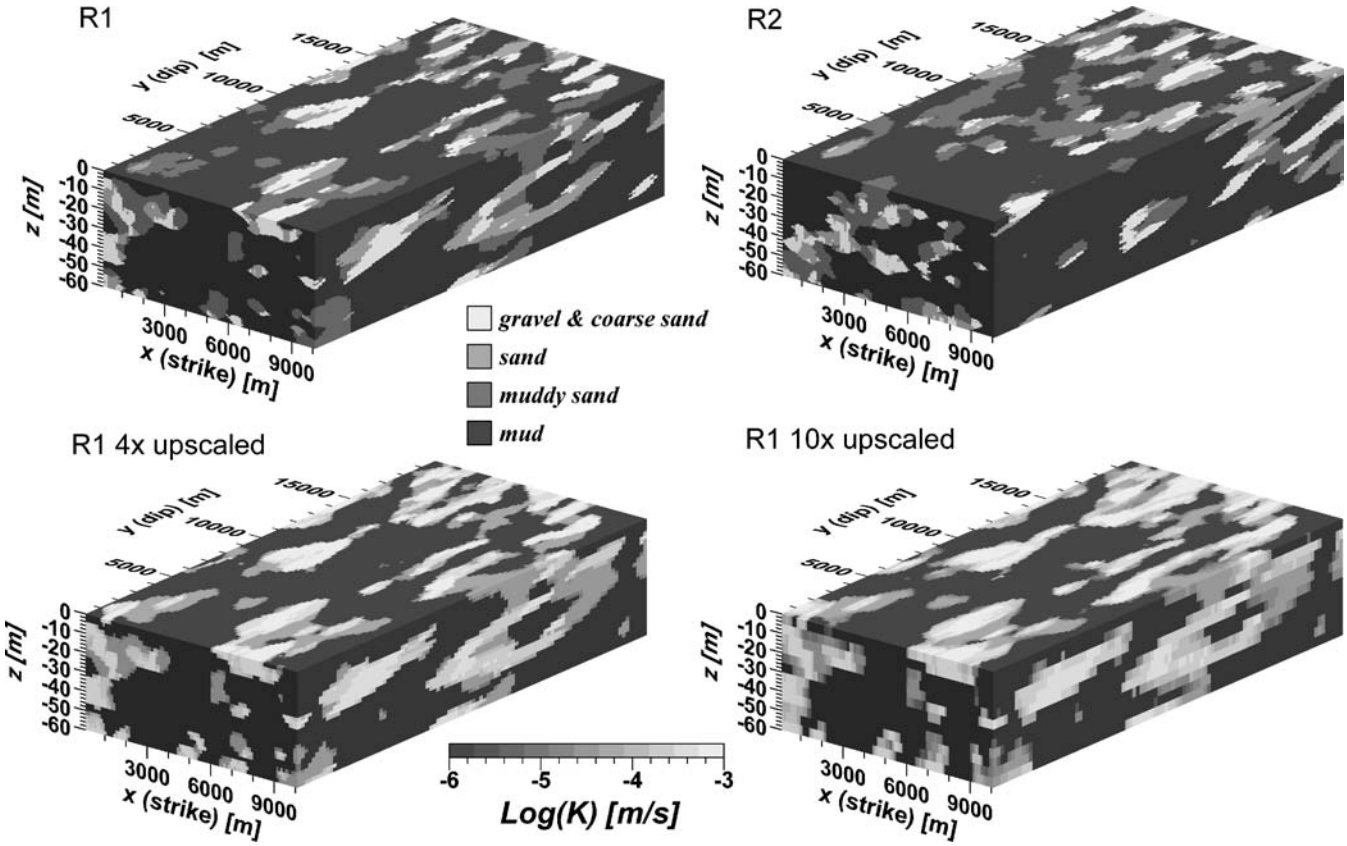

Fig. 1 Subdomains from *R1* and *R2* of the five realizations of the geostatistical model and *R1 upscaled 4x* and *10x*. The original model has 120 layers (1,224,000 cells) and the upscaled models 30 layers (30,6000 cells) and 12 layers (122,400 cells) respectively

hydrofacies based on data from the field and the literature (see Fleckenstein 2004).

Upscaling procedure

Upscaling was performed in a two-step procedure in which upscaled values were first estimated via Wiener bounds and then corrected to account for loss of information on connectivity. In the initial step hydrofacies, *K*-values were averaged over sections of vertical grid columns of the geostatistical model (see also Fig. 4). A specific number of layers of the original model (120 layers) was averaged within each grid column. The degree of upscaling is expressed as the number of layers that are upscaled into one larger block within the grid columns or as the percent fraction of the entire model thickness that is upscaled.

Equivalent horizontal hydraulic conductivity ($K_{eq,xy}$) was upscaled using the weighted arithmetic mean of the hydrofacies *K*-values (Table 1). To calculate equivalent vertical hydraulic conductivity ($K_{eq,z}$), the weighted harmonic mean was used. The upscaled *K*-values therefore represent the exact equivalent *K* for local conditions of flow parallel (horizontal direction) and perpendicular (vertical direction) to the layering subject to uniform boundary conditions within each upscaled grid block. This procedure was applied to the five realizations. *K*-values were upscaled over 2, 3, 4, 5, 6, 8, 10, 20, 40, 60 and 120 grid layers (1.7, 2.5, 3.3, 4.2, 5.0, 6.7, 8.3, 20, 33.3, 50 and 100%).

Table 1 *K*-values assigned to the four hydrofacies

Hydrofacies (alluvial setting)	Description	Saturated hydraulic conductivity (m/s)
I (channel)	Gravel and coarse sand	1.00E-03
II (channel)	Sand	5.00E-04
III (near channel)	Muddy sand	5.00E-05
IV (floodplain)	Mud	1.50E-06

Numerical experiments (upscaling effects at the domain-scale)

To assess the effects of the described upscaling on K_{eq} at the scale of the entire model domain, numerical flow simulations were conducted. Flow on the scale of the model domain also depends on how hydrofacies are juxtapositioned between adjacent grid cells and how high *K* hydrofacies are connected throughout the entire model domain (Fogg et al. 2000; Knudby and Carrera 2005; Knudby et al. 2006).

In the numerical experiments, equivalent *K* was determined from simulations of steady-state groundwater flow through the original and upscaled subdomains. The USGS groundwater flow code MODFLOW2000 (McDonald and Harbaugh 1988; Harbaugh et al. 2000) was used by applying specified head boundaries on two sides of the

 DOI 10.1007/s10040-008-0312-3

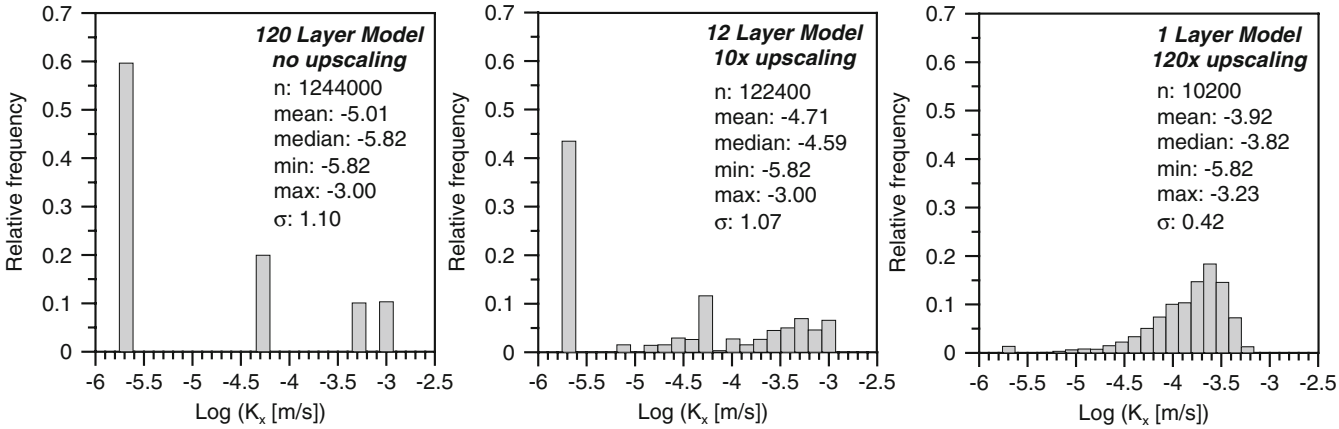

Fig. 2 Histograms of Log(K_{xy}) at different degrees of upscaling for R1—K_x=K_y because no lateral upscaling is performed

domain and no-flow boundaries on all other sides. Simulations were carried out in the dip- (y), strike- (x) and vertical- (z) directions. The imposed hydraulic gradients across the domain in the dip-, strike- and vertical directions were 0.00151, 0.00446 and 0.01513, respectively. The head tolerance in MODFLOW was set to 0.0001 m. Absolute mass balance errors were below 0.1% for all simulations. To check for possible errors caused by numerical discretization, the upscaled coarse models from one realization of the geostatistical model were mapped back to the original fine-scale grid and the same simulations were run again for the dip direction. Relative differences in flow between the coarse and fine grids ranged from 0 to only 0.9%, indicating that numerical errors are negligible with respect to regional flow, and hence computed equivalent *K*.

From the flow simulations, upscaling functions were derived that describe the change in equivalent *K* of the entire model domain as a function of the degree of upscaling. Effects of the different structural arrangements of hydrofacies in the model domain on K_{eq} were evaluated by running the same steady-state flow simulations for five realizations of three different geostatistical models that represent *K*-fields, which had almost identical mean, variance and covariance structure as the original geostatistical model, but a different spatial arrangement of the hydrofacies.

Results and discussion

K-distributions

Figure 2 shows histograms of the log(K_{xy})-distribution in the original and upscaled domains. In the original model, only four distinct *K*-values are present, one for each of the four hydrofacies. With increasing upscaling the distinct four modes of the original distribution disappear. At the 10× upscaling degree, two of the four original modes are still clearly visible, the other two only vaguely visible. At the 120× degree, all original modes in the distribution are lost. The distinct mode from a specific hydrofacies in the *K*-distribution starts to disappear at upscaling degrees that are equivalent to length scales of about 1–2 times the mean thickness of that hydrofacies (Fig. 2). At upscaling degrees of 10×, for example, which is equivalent to a length scale of 5 m (10×0.5 m cell thickness), the distinct mode of the gravel and coarse sand hydrofacies (mean length in the vertical = 3.93 m, see Table 3) in the *K*-distribution (at log(K_{xy}) = –3) starts to fade into a more continuous *K*-distribution.

At degrees of upscaling < = 10× the main characteristics of the original *K*-distribution (peaks, mean, range, median, standard deviation) are still preserved. At larger degrees of upscaling (e.g. 120×, i.e. all 120 layers of the original grid are upscaled into one single layer), in contrast, the log(K_{xy})-distribution resembles few characteristics of the original distribution. At 120× upscaling, the distribution becomes unimodal with the mode in the high-*K* rather than in the low-*K* range of the dominant floodplain hydrofacies. The shift of the mode is caused by the bias of the arithmetic mean for high-*K* values, which are increasingly sampled at large degrees of upscaling.

Generally it can be said that at degrees of upscaling up to the scale of the mean vertical length of the hydrofacies, the upscaled model grid still mainly consists of bodies that are characterized by the distinct four hydrofacies *K*-values with zones of intermediate *K* between the bodies. This effect is demonstrated in the lower portion of Fig. 1. Whereas the overall spatial arrangement of hydrofacies bodies is largely preserved at low degrees of upscaling, the sharp boundaries between bodies in the original model are progressively smoothed. For example, the spatial arrangement and shapes of the alluvial channel hydrofacies bodies (light colors) are hardly changed but slightly blurred at the edges. This suggests that large reductions in problem-size can be achieved with the proposed method without significantly compromising the representation of overall geologic structure.

Upscaling effects on model domain equivalent K_{xy}

Effects of the suggested upscaling method on equivalent, lateral and vertical *K*-values ($K_{eq,xy}$ and $K_{eq,z}$) at the scale

 DOI 10.1007/s10040-008-0312-3

of the model domain were investigated with numerical flow simulations. In Fig. 3, model domain equivalent K for R1–R5 are plotted versus the degree of upscaling for the dip- and strike- directions. The vertical direction is addressed in a subsequent paragraph. The arithmetic mean of the four hydrofacies K-values weighted by their volumetric proportions, which represents the upper bound for K_{eq} is shown as a dashed line. Maximum values of $K_{eq,xy}$ (in the dip-direction) were close to the arithmetic mean, which is in accordance with other studies on three-dimensional (Fogg et al. 2000) and two-dimensional K-fields (Zhang et al. 2007)

All five realizations show an increase of K_{eq} with progressive degrees of upscaling. A similar increase in equivalent K for local upscaling in the vertical was reported by Wen et al. (2003). For all realizations K_{eq} increases rapidly up to about the 10% upscaling degree and then levels off. This behavior fits a logarithmic function of the form:

$$y = A \cdot Log(x) + B \tag{2}$$

The coefficient of determination (R^2) was larger than 0.99 for all realizations in the dip-direction and larger than 0.96 for all realizations in the strike-direction. The same function could be used to describe the relative error in equivalent K (compared to actual K), which was found to be practically identical for the different realizations of the heterogeneity model (unique coefficients A and B). P-norms (Eq. 1) in the original models ranged from 0.74 to 0.82 in dip-direction and from 0.52 to 0.64 in the strike-direction. Over the various degrees of upscaling the range increased to 0.75–0.95 in the dip- and 0.54–0.76 in the strike-direction. Absolute values of K_{eq} are different between different realizations. As a result, the upscaling functions are shifted along the ordinate axis. These shifts are probably the result of differences in connectivity of the high-K hydrofacies between realizations. The same effect is visible in the overall lower K_{eq} in the strike-direction. The high-K channel bodies have significantly longer mean length in the dip-direction, which results in better connectivity in that direction.

These results suggest that for a stationary geostatistical hydrofacies model with distinct spatial statistics, the relative change in lateral K (dip and strike) due to a given degree of upscaling is unique and does not significantly vary between different realizations of the model. In other words, a unique upscaling function for a geostatistical model with defined spatial statistics can be developed from a single realization of the model. For the model investigated here, this function takes a logarithmic form (Eq. 2) and can be used to correct the upscaled K-field for scaling effects. This correction will be elaborated in more detail in a later paragraph. The parameters A and B in Eq. 2 can be estimated from curve fitting of results from flow simulations of the type described above. Once the upscaling relationship is determined for one realization of the specific geostatistical model, it can be applied to any other realization of that model. In this way, a large number of realizations of a geostatistical heterogeneity model, e.g. in a Monte Carlo analysis, can be upscaled very efficiently.

It is important to consider what causes the consistent increase in K_{eq} at increasing degrees of upscaling and what determines the specific shape of the upscaling function, i.e. the values of A and B in Eq. 2. For the latter question, it is hypothesized that the shape of the upscaling function is defined by the connectivity of high-K hydrofacies in the geostatistical model, which will be discussed later in the paper. The increase in K_{eq} with increasing upscaling is caused by artificially enhanced

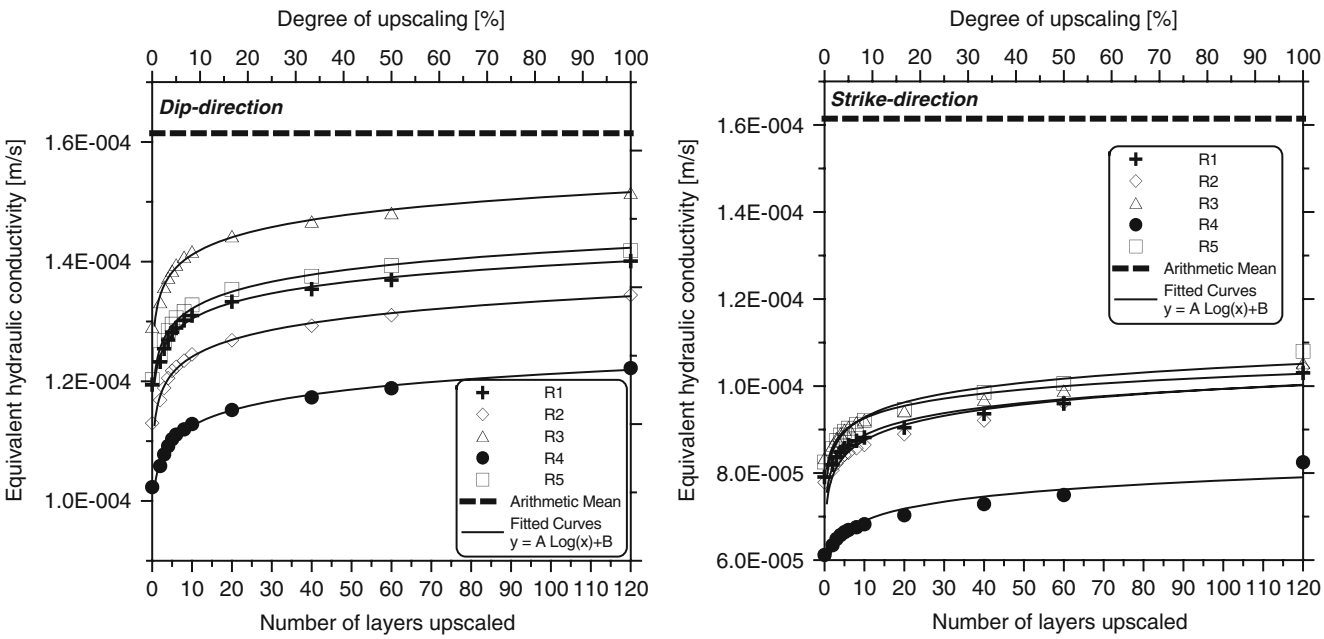

Fig. 3 Effects of upscaling on model domain equivalent K in the dip- (y) and strike- (x) directions for five different realizations of the geostatistical model

 DOI 10.1007/s10040-008-0312-3

connectivity between adjacent grid columns, as demonstrated in Fig. 4.

In this example, two adjacent grid columns consisting of ten layers are made up of a mix of high-*K* material (e.g. sand) and a low-*K* material (e.g. mud). All high-*K* cells lie next to low–*K* cells. Lateral flow between the two columns is therefore limited by the low-*K* material. No direct high–*K* connections exist between the two columns. If the ten cells are upscaled with the methodology presented here, the resulting *K*-values of the upscaled columns will lie between the *K*-values of the original two materials. Hence the lowest *K* in the upscaled column is larger than the lowest *K* in the original columns, causing artificially high lateral flow between the two columns. Although the above example is based on a binary medium, the same concept applies to a medium with more than two hydrofacies. In other words, the proposed upscaling procedure would always result in increased lateral flow connectivity between adjacent model columns due to an increase in the minimum *K* limiting flow between the two columns. A similar line of argument was used by Wen et al. (2003) to explain a positive bias in equivalent *K* obtained from local averaging of a binary medium in the vertical. If the length-scale of the upscaling exceeds the scale of the mean thickness of the hydrofacies (in particular the high-*K* facies), the effect of increased connectivity will diminish, because the upscaling procedure starts to include data beyond the correlation length of the hydrofacies. This effect explains the leveling off of the upscaling function. The artificial increase in equivalent *K* is a result of the local nature of the heuristic method used and of upscaling in the vertical only. If *K* had also been averaged in the lateral directions, the resulting equivalent *K* might be smaller than the actual value. Wen et al. (2003) suggested the use of border regions to reduce the bias of local upscaling on equivalent K. They later used this approach in an iterative local-global upscaling technique for three-dimensional reservoir simulation (Wen et al. 2006). This method, however, is computationally very expensive if multiple realizations of a heterogeneity model are to be upscaled. Therefore a simple empirical correction based on curve fitting, which will be described below, was used here to remove local biases.

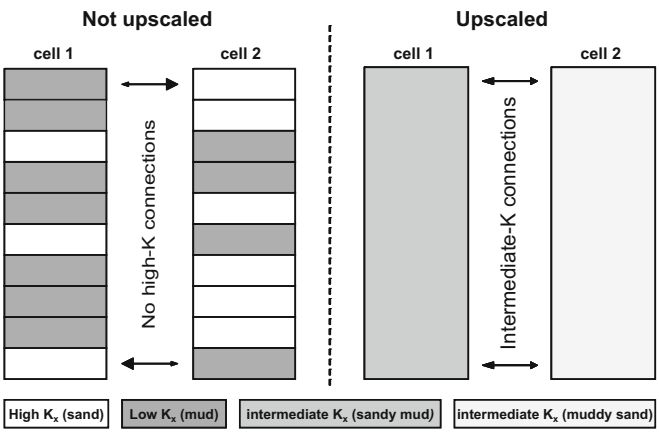

Fig. 4 Effects of upscaling on flow connections between model blocks. *Arrows* indicate flow between cells, size of the *arrow heads* indicates the ease at which water can flow into the adjacent cell

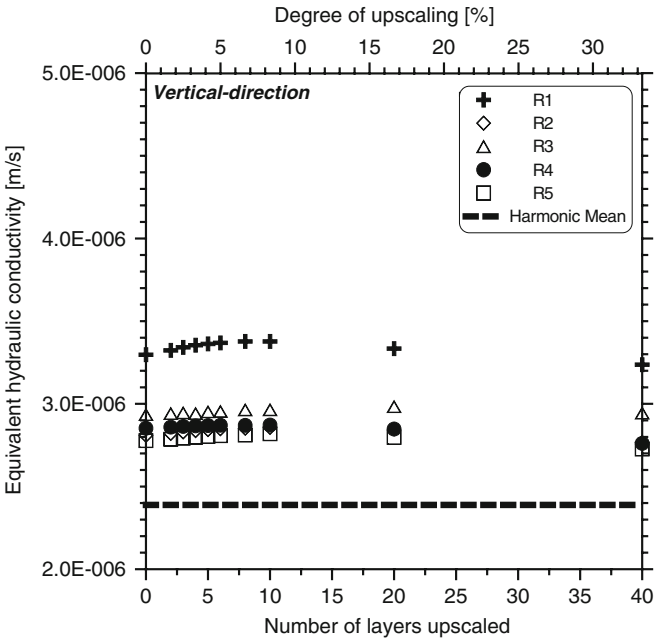

Fig. 5 Effects of upscaling on $K_{eq,z}$ for *R1–R5*

Upscaling effects on model domain equivalent K_z

$K_{eq,z}$ was relatively insensitive to upscaling (Fig. 5). Because harmonic averaging, which was used to upscale in the vertical-direction, weights low-*K*-values more than high-*K* values, the upscaling did not significantly increase vertical flow connectivity. In fact, vertical model domain equivalent *K* ($K_{eq,z}$) practically did not change with increasing degree of upscaling.

Correction of upscaled *K*-fields

The upscaling functions derived from the numerical experiments were then used to correct the upscaled *K*-fields so that net lateral flow through the upscaled domain was the same as through the original model. *K*-values were adjusted by multiplying individual cell *K*-values by a correction factor, which was calculated from the following equation:

$$F_{corr.} = 1 - \frac{Err}{100 + Err} = \frac{100}{100 + Err} \qquad (3)$$

where Err is the relative error in equivalent *K* in % between the original and the upscaled models, which was calculated from the logarithmic upscaling function. Flow through the corrected *K*-fields was then simulated to check, if flow through the corrected, upscaled models was the same as through the original model.

Figure 6 shows the relative error in net-flow in the dip-direction for the original and corrected upscaled fields as a

DOI 10.1007/s10040-008-0312-3

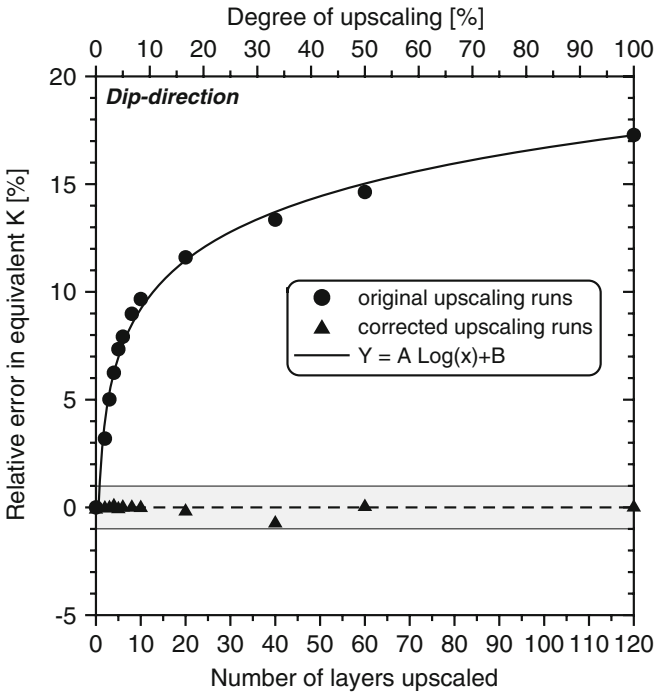

Fig. 6 Effects of scaling-correction of the *K*-field on the relative error in $K_{eq,xy}$ in the dip-direction for realization 1. The *grey-shaded area* marks the 1% error margin

function of the degree of upscaling. Upscaling corrections generally reduced errors in K_{eq} to values below 1%. Similar error ranges (0–1%) were found for the strike-direction and for different realizations of the geostatistical model.

Connectivity of high-*K* facies and its relationship to $K_{eq,xy}$

It is well known that in the absence of geologic discontinuities such as faults or unconformities, geologic facies that comprise at least 18% of the system volume will tend to percolate or form connected pathways in three-dimensions (Fogg et al. 2000; Harter 2005; Weissmann and Fogg 1999). Although the importance of connectivity for subsurface flow and transport has long been recognized (Fogg 1986; Western et al. 1998, 2001, Knudby 2004; Lee et al. 2007), it is difficult to quantify. In fact, no standardized methods exist to characterize connectivity. Most conventional geostatistical measures only poorly capture connectivity (Western et al. 1998, 2001; Knudby and Carrera 2005). To test the hypothesis that differences in $K_{eq,xy}$ between the different realizations of the geostatistical model, reflected in the shift of the upscaling curves along the ordinate in Fig. 3, are caused by differences in the connectivity of the high-*K* hydrofacies several indicators of connectivity were determined, which could be compared between different realizations of the geostatistical model.

It was found that the gravel and sand hydrofacies, which make up about 20% of the domain, jointly percolated the entire length of the domain in the dip-, strike- and vertical-directions in all realizations except R2. This is in agreement with recent studies, which found percolation thresholds in three-dimensional binary and multi-categorical fields at volumetric proportions between 15 and 20% (Lee 2004; Harter 2005). Because differences in K_{eq} could not be inferred from the joint percolation of the gravel and sand hydrofacies, three alternative indicators based on the gravel hydrofacies alone were identified: percentage of domain lengths traversed by the longest connected body consisting of hydrofacies 1 (I_1), the number of bodies percolating 1/2 of the domain length (I_2), and the number of bodies percolating 1/3 of the domain length (I_3). These indicators are listed in Table 2 for the dip- and strike-directions for R1–R5.

In both the dip- and strike-directions, the realization with the longest connected body of hydrofacies 1 also had the highest K_{eq}. To determine if the calculated connectivity indicators could explain the ranking in K_{eq}, a multiple regression analysis was conducted. The regression equation is:

$$K_{eff,xy} = a_1 I_1 + a_2 I_2 + a_3 I_3 + a_0 \quad (4)$$

where $K_{eq,xy}$ is the model domain equivalent K in the lateral directions, I_1, I_2 and I_3 are the three connectivity indicators from Table 2, a_1, a_2 and a_3 are the coefficients and a_0 the intercept of the regression equation. R^2-values

Table 2 Quantitative indicators for connectivity of hydrofacies 1 (gravel) in the dip- and strike- directions (numbers in brackets are ranks)

Realization	Equivalent model domain K (m/s)	Longest connected body in % of domain length (I_1)	Number of bodies percolating 1/2 of domain length (I_2)	Number of bodies percolating 1/3 of domain length (I_3)
Dip-direction				
R1	1.183E-04 (3)	90 (2)	2 (2)	8 (1)
R2	1.119E-04 (4)	88 (4)	2 (2)	7 (2)
R3	1.278E-04 (1)	100 (1)	1 (3)	5 (3)
R4	1.013E-04 (5)	63 (5)	1 (3)	7 (2)
R5	1.191E-04 (2)	89 (3)	3 (1)	7 (2)
Strike-direction				
R1	7.832E-05 (3)	46 (5)	0 (3)	2 (3)
R2	7.709E-05 (4)	67 (2)	1 (2)	3 (2)
R3	8.268E-05 (1)	85 (1)	1 (2)	3 (2)
R4	6.059E-05 (5)	47 (4)	0 (3)	2 (3)
R5	8.174E-05 (2)	53 (3)	2 (1)	4 (1)

 DOI 10.1007/s10040-008-0312-3

Table 3 Embedded transition probability matrices and mean hydrofacies lengths (diagonal terms) in the vertical direction for the original (MA) and the two additional TPROGS models MC and MD

Original model MA

	g	*sd*	*ms*	*m*
g	$\overline{L} = 3.93m$	0.40	0.30	*b*
sd	0.1	$\overline{L} = 2.84m$	0.45	*b*
ms	0.1	0.3	$\overline{L} = 5.68m$	*b*
m	*b*	*b*	*b*	*b*

Model MC

	g	*sd*	*ms*	*m*
g	$\overline{L} = 20.00m$	0.40	0.30	*b*
sd	0.1	$\overline{L} = 20.00m$	0.45	*b*
ms	0.1	0.3	$\overline{L} = 5.68m$	*b*
m	*b*	*b*	*b*	*b*

Model MD

	g	*sd*	*ms*	*m*
g	$\overline{L} = 1.00m$	0.60	0.30	*b*
sd	*s*	$\overline{L} = 1.00m$	0.30	*b*
ms	*s*	*s*	$\overline{L} = 5.68m$	*b*
m	*b*	*b*	*b*	*b*

g gravel and coarse sand; *sd* sand; *ms* muddy sand; *m* mud; *s* symmetry; *b* background category

of the multiple regression were 0.92 for the dip-direction and 0.53 for the strike-direction showing that the indicators are better predictors of the $K_{eq,y}$ than $K_{eq,x}$. More than 90% of the variance in $K_{eq,y}$ is explained by its linear relation with the three indicators. For the less connected strike-direction ($K_{eq,x}$) it is only 53%. These results suggest that there is a significant correlation between the connectivity of high-K hydrofacies and $K_{eq,xy}$ of the system.

Mean length, structure and the upscaling relationship

It has been previously hypothesized that the shape of the upscaling function largely depends on the specific spatial structure of the K-field. Yong (2004) found that upscaling of three-dimensional indicator fields was strongly controlled by the global volumetric proportions and mean K of the hydrofacies as well as connectivity parameters. To test if the geometry (defined by the mean

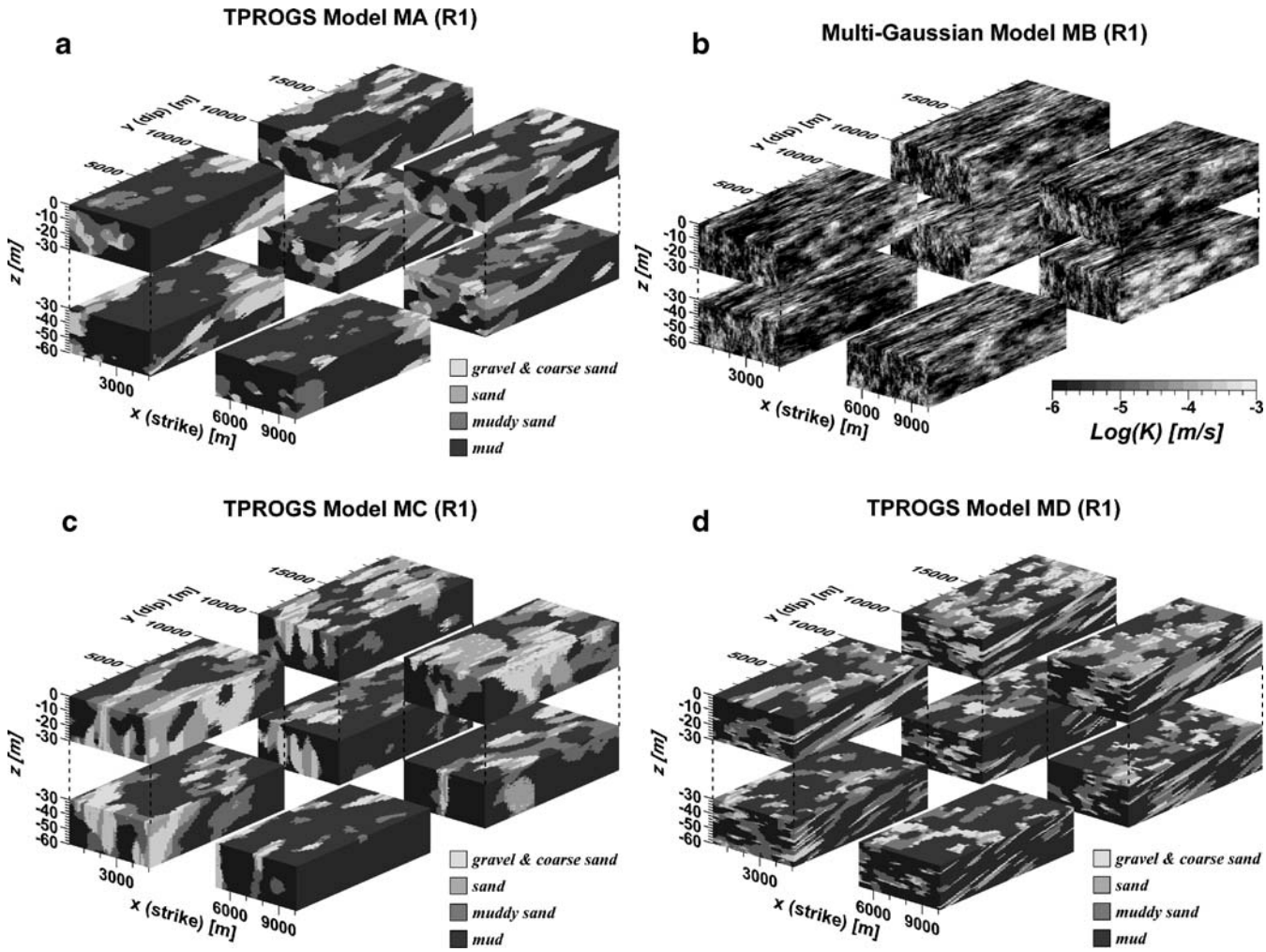

Fig. 7 Four different subsurface models—**a** MA, **b** MB, **c** MC and **d** MD—with the same mean, variance and covariance structure in hydraulic K representing different spatial arrangements of hydrofacies. Vertical exaggeration ~90×

 DOI 10.1007/s10040-008-0312-3

length and thickness) and structure (defined by connectivity) of the high-K hydrofacies could explain the different shapes of the upscaling curves, the upscaling procedure was applied to two more sets of K-fields consisting of five realizations each that had the same mean and variance as the original K-fields but differed in the mean thickness of the two high-K hydrofacies. The fields were created with TPROGS by changing the mean length of the high-K hydrofacies in the embedded transition probability matrices for the vertical-direction (Table 3; Fig. 7).

In the first alternative model (MC), mean thicknesses for the gravel and sand hydrofacies were set to 20.00 m instead of 3.93 and 2.84 m in the original model. In the second model (MD), mean thicknesses of 1.00 m were chosen for those hydrofacies. The two resulting models have the same volumetric proportions of hydrofacies and the same mean and variance in their K distributions as the original model, but differ in the shape and structure of their high-K hydrofacies (channel facies). Model MC (larger mean lengths) is characterized by thicker and fewer channel bodies, whereas model MD (shorter mean lengths) shows a larger number of thinner channel bodies than the original model (Fig. 7).

For further comparison, five realizations of a multi-Gaussian model (MB) were created with the code SGSIM from the Geostatistical Software Library (GSLIB; Deutsch and Journel 1998). The model of spatial correlation was based on a variogram analysis of a K-distribution sampled from realization 1 of the original geostatistical model. This was done to produce a multi-Gaussian model that is statistically identical to the TPROGS models (same mean and variance), but with less of the hydrofacies-style geologic structuring.

After the upscaling procedure had been applied to the additional K-fields, the same steady-state flow experiments that had been conducted with the original geostatistical model were done with the new fields. Figure 8 shows the upscaling curves for the additional K-fields in comparison to the original hydrofacies model. All models show similar upscaling behavior, the difference in $K_{eq,y}$ between the upscaled and not upscaled models grows with the degree of upscaling. Just as for the original model, the curves all show a logarithmic shape and are almost identical between different realizations of a specific model.

In model d (MD), flow connectivity is already significantly increased at low degrees of upscaling, because channel bodies are thin (shorter mean length) and upscaling starts to affect flow connectivity between adjacent cell blocks at short length-scales. In contrast, in model c (MC), which is characterized by a smaller number of thick channel bodies (larger mean length), effects of upscaling on flow are smaller at low degrees of upscaling. The upscaling behavior of the original model, which has an intermediate mean length of the channel hydrofacies, lies between these two models. For flow through the multi-Gaussian model, which represents K-fields with a large degree of randomness (given the imposed statistical

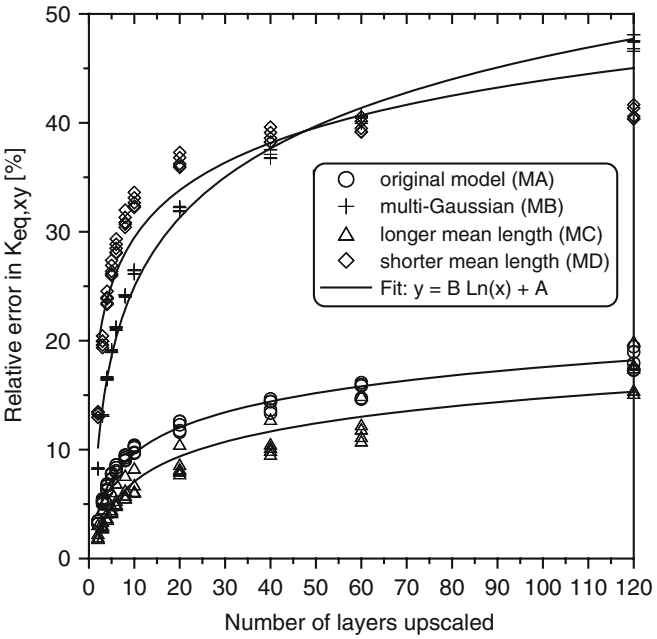

Fig. 8 Upscaling curves for the different subsurface models (*MA*, *MB*, *MC* and *MD*) and their associated K-fields with same mean and variance but different spatial structure

structure), the effects of upscaling are more pronounced. The arithmetic averaging in the upscaling procedure significantly increases flow connectivity between cell blocks in the relatively unstructured multi-Gaussian fields. The relative error in K_{eq} increases rapidly with the degree of upscaling.

These results show that the upscaling function is strongly affected by the spatial arrangement of high-K zones or hydrofacies in the system. This arrangement in turn is determined by the statistical structure of the subsurface model. Multiple linear regressions of the same connectivity indicators used in the previous paragraph with equivalent K in the dip-direction yielded similarly high R^2 values of 0.92 for MC and 0.91 for MD respectively. Upscaling methods should account for the connectivity of high-K zones and how connectivity is affected by the upscaling method. These effects are important for groundwater flow and even more so for simulations of transport (Scheibe and Yabusaki 1998; Knudby and Carrera 2005).

Summary and conclusions

An upscaling procedure for hydraulic K of subsurface hydrofacies as described by a detailed three-dimensional geostatistical indicator simulation was developed. The method is based on arithmetic and harmonic averaging of hydrofacies K-values within vertical sections of grid columns and application of a correction factor that preserves the correct flow volumes over the greater model domain. The methodology was applied to four different geostatistical K-fields reflecting different structures of high-K zones and five realizations each. Effects of

 DOI 10.1007/s10040-008-0312-3

upscaling on K_{eq} were investigated by means of numerical simulation of steady-state flow.

The numerical flow simulations showed an increase of K_{eq} with increasing degrees of upscaling. For all realizations of each geostatistical model, the increase was uniquely described by a logarithmic function. This function could be used to correct the upscaled K-fields for the non-local effects of scaling. Differences in the absolute values of K_{eq} between different realizations could be explained with the level of connectivity of the high-K hydrofacies.

The parameters of the logarithmic function were found to be dependent on the structure of the K fields. Fields containing a large number of thin channel bodies reacted more strongly to increasing degrees of upscaling, whereas fields with fewer but thicker channel bodies reacted with a smaller increase in equivalent K. Flow through the multi-Gaussian fields, which display a larger level of disorder, reacted most strongly to increasing upscaling.

The presented procedure allows a fast and efficient upscaling of K-fields resulting from multiple realizations of a three-dimensional geostatistical hydrofacies model with a unique upscaling function, which can be derived from a flow simulation carried out on a single realization of the geostatistical model. The parameters of the function appear to be unique for the specific geostatistical model they were derived from. The effects of transient flow and variable boundary conditions on the proposed methodology have not been fully tested yet. Several authors have reported effects of varying boundary conditions on equivalent K (Gomez-Hernandez and Gorelick 1989; Paleologos et al. 1996; Dagan and Neuman 1997). Zhang et al. (2006, 2007), in some recent work on a large regional flow system, however, found minor effects of variable boundary conditions on equivalent K and concluded a possible emergence of an effective K for large flow systems. The proposed methodology has already been applied to a large transient problem of river–aquifer interactions using a correction factor obtained from the steady-state simulations presented here (Fleckenstein et al. 2006). In that study, the upscaled model could not be compared to a transient simulation of the original fine-scale model because of computational limitations, but it was able to adequately represent the observed hydrologic dynamics and pressure distributions of the system at an intermediate scale (not just at the global scale). That hints at a possibly broader applicability of the methodology. However, the full effects of transient flow and variable boundary conditions, as well as effects of the specific K-values assigned to the hydrofacies and the contrast between them, need to further be investigated in the future. Finally, it should be stressed that the effects of local heuristic upscaling on transport (e.g. equivalent dispersivity) might be quite different from the effects on flow. It remains to be seen if similar correction functions could be developed for transport.

Acknowledgements The authors would like to thank CALFED for their funding through the California Bay-Delta Authority's Ecosystem Restoration Program: Grants ERP No. 99-NO6 and ERP No. 01-NO1. The helpful comments and suggestions from the managing editor, three anonymous reviewers and Christen Knudby were also greatly appreciated.

References

Ababou R, McLaughlin D, Gelhar LW, Tompson AFB (1989) Numerical-simulation of 3-dimensional saturated flow in randomly heterogeneous porous-media. Transp Porous Media 4 (6):549–565

Carle SF (1999) TPROGS: transition probability geostatistical software, version 2.1, user manual. Hydrologic Sciences Graduate Group, University of California, Davis, USA

Carle SF, Fogg GE (1996) Transition probability-based indicator geostatistics. Math Geol 28(4):453–476

Carle SF, Fogg GE (1997) Modeling spatial variability with one and multidimensional continuous-lag Markov chains. Math Geol 29 (7):891–918

Carle SF, La Bolle EM, Weissmann GS Van Brocklin D, Fogg GE (1998) Conditional simulation of hydrofacies architecture: a transition probability/Markov approach. In: Fraser GS, Davis JM (eds) Hydrogeologic models of sedimentary aquifers. Concepts in Hydrogeology and Environmental Geology, SEPM Spec Publ 1:147–170

Chen Y, Durlofsky LJ Gerritsen M, Wen XH (2003) A coupled local-global upscaling approach for simulating flow in highly heterogeneous formations. Adv Water Resour 26:1041–1060

Cushman JH, Bennethum LS, Hu BX (2002) A primer on upscaling tools for porous media. Adv Water Resour 25:1043–1067

Dagan G (2001) Effective, equivalent and apparent properties of heterogeneous media. In: Aref H, Phillips JW (eds) Mechanics for a new millennium: Proceeding of the 20th International Congress on Theoretical and Applied Mechanics. Kluwer, Dordrecht, pp 473–485

Dagan G, Neuman SP (1997) Subsurface flow and transport: a stochastic approach. University Press, Cambridge

de Marsily G, Delay F, Teles V, Schafmeister MT (1998) Some current methods to represent the heterogeneity of natural media in hydrogeology. Hydrogeol J 6:115–130

de Marsily G, Delay F, Goncalves J, Renard P, Teles V, Violette S (2005) Dealing with spatial heterogeneity. Hydrogeol J 13(1):61–183

Desbarats AJ (1994) Spatial averaging of hydraulic conductivity under radial flow conditions. Math Geol 26:1–21

Deutsch CV, Journel AG (1998) GSLIB: geostatistical software library and user's guide. Oxford University Press, New York

Eaton TT (2006) On the importance of geological heterogeneity for flow simulation. Sediment Geol 184(3–4):187–201

Fiori A, Jankovic I, Dagan G (2003) Flow and transport through two-dimensional isotropic media of binary conductivity distribution, part 1: numerical methodology and semi-analytical solutions. Stoch Environ Res Risk Assess 17:370–383

Fleckenstein JH (2004) Modeling river-aquifer interactions and geologic heterogeneity in an alluvial fan system, Cosumnes River, CA. PhD Thesis, Hydrologic Sciences Graduate Group, University of California, Davis, USA

Fleckenstein JH, Niswonger RG, Fogg GE (2006) River-aquifer interactions, geologic heterogeneity, and low-flow management. Ground Water 44:837–852

Fogg GE (1986) Groundwater-flow and sand body interconnectedness in a thick, multiple-aquifer system. Water Resour Res 22(5):679–694

Fogg GE, Carle SF, Green CT (2000) Connected-network paradigm for the alluvial aquifer system. In: Zhang D, Winter CL (eds) Theory, modeling and field investigation in hydrogeology: a special volume in honor of Shlomo P. Neuman's 60th birthday, Geological Society of America Spec Pap 348, pp 25–42

Gomez-Hernandez JJ, Gorelick SM (1989) Effective groundwater model parameter values: influence of spatial variability of hydraulic conductivity, leakance and recharge. Water Resour Res 25(3):405–419

Harbaugh AW, Banta ER, Hill MC, McDonald MG (2000) MODFLOW-2000, The US Geological Survey Modular ground-water model: user guide to modularization concepts and the ground-water flow process, US Geol Surv Open-File Rep 00–92

Harter T (2005) Finite-size scaling analysis of percolation in three-dimensional correlated binary Markov chain random fields. Phys Rev E Stat Nonlin Soft Matter Phys 72(2), 026120

Indelman P (2003) Transient well-type flows in heterogenous formations. Water Resour Res 39(3), 1064. 10.1029/2002WR001407

Jankovic I, Fiori A, Dagan G (2003) Effective conductivity of an isotropic heterogeneous medium of lognormal conductivity distribution. Multiscale Model Simul 1:40–56

Journel AG (1996) Conditional simulation of geologically averaged block permeabilities. J Hydrol 183(1–2):23–35

Journel AG, Deutsch CV, Desbarats AJ (1986) Power averaging for block effective permeability. Paper presented at 56th California regional meeting of the Society of Petroleum Engineers, Oakland, CA, April 1986

Knudby C (2004) On the concept of hydrogeologic connectivity. PhD Thesis, Technical University of Catalonia, Spain

Knudby C, Carrera J (2005) On the relationship between indicators of geostatistical, flow and transport connectivity. Adv Water Resour 28(4):405–421

Knudby C, Carrera J, Bumgardner JD, Fogg GE (2006) Binary upscaling: the role of connectivity and a new formula. Adv Water Resour 29:590–604

Koltermann CE, Gorelick SM (1996) Heterogeneity in sedimentary deposits: a review of structure-imitating, process-imitating, and descriptive approaches. Water Resour Res 32(9):2617–2658

LaBolle EM, Fogg GE (2001) Role of molecular diffusion in contaminant migration and recovery in an alluvial aquifer system. Transp Porous Media 42(1–2):155–179

Lee SY (2004) Heterogeneity and transport: geostatistical modeling, non-Fickian transport, and efficiency of remediation methods. PhD Thesis, University of California, Davis, USA, 267 pp

Lee SY, Carle SF, Fogg GE (2007) Geologic heterogeneity and a comparison of two geostatistical models: sequential Gaussian and transition probability-based geostatistical simulation. Adv Water Resour 30:1914–1932

McDonald MG, Harbaugh AW (1988) A modular three-dimensional finite-difference ground-water flow model. USGS Techniques of Water-Resources Investigations, Book 6, Chapter A1, US Geological Survey, Reston, VA

Neuman SP, Di F (2003) Multifaceted nature of hydrogeologic scaling and its interpretation. Rev Geophys 41(3), 1014. DOI 10.1029/2003RG000130

Noetinger B, Artus V, Zargar G (2005) The future of stochastic and upscaling methods in hydrogeology. Hydrogeol J 13(1):84–201

Paleologos EK, Neuman SP, Tartakovsky D (1996) Effective hydraulic conductivity of bounded, strongly heterogeneous porous media. Water Resour Res 32:1333–1341

Pozdniakov S, Tsang CF (2004) A self-consistent approach for calculating the effective hydraulic conductivity of a binary, heterogeneous medium. Water Resour Res 40, W05105. DOI 10.1029/2003WR002617

Renard P, de Marsily G (1997) Calculating equivalent permeability: a review. Adv Water Resour 20(5–6):253–278

Renard P, Le Loch G, Ledoux E, de Marsily G, Mackay R (2000) A fast algorithm for the estimation of the equivalent hydraulic conductivity of heterogeneous media. Water Resour Res 36 (12):3567–3580

Ritzi RW, Jayne DF, Zahradnik AJ, Field AA, Fogg GE (1994) Geostatistical modeling of heterogeneity in glaciofluvial, buried-valley aquifers. Ground Water 32(4):666–674

Robin MJL, Gutjahr AL, Sudicky EA, Wilson JL (1993) Cross-correlated random field generation with the direct Fourier transform method. Water Resour Res 29(7):2385–2397

Rubin Y (1995) Flow and transport in bimodal heterogeneous formations. Water Resour Res 31:2461–2468

Sanchez-Vila X, Guadagnini A, Carrera J (2006) Representative hydraulic conductivities in saturated groundwater flow. Rev Geophys 44(3), RG3002. DOI 10.1029/2005RG000169

Scheibe T, Yabusaki S (1998) Scaling of flow and transport behavior in heterogeneous groundwater systems. Adv Water Resour 22 (3):223–238

Tartakovsky DM, Guadagnini A (2004) Effective properties of random composites. Siam J Sci Comput 26:625–635

Tartakovsky DM, Neuman SP (1998) Transient effective hydraulic conductivities under slowly and rapidly varying mean gradients in bounded three-dimensional random media. Water Resour Res 34:21–32

Tompson AFB, Carle SF, Rosenberg ND, Maxwell RM (1999) Analysis of groundwater migration from artificial recharge in a large urban aquifer: a simulation perspective. Water Resour Res 35(10):2981–2998

Webb EK (1995) Simulation of braided channel topology and topography. Water Resour Res 31(10):2603–2611

Webb EK, Anderson MP (1996) Simulation of preferential flow in three-dimensional, heterogeneous conductivity fields with realistic internal architecture. Water Resour Res 32(3):533–545

Weissmann GS, Fogg GE (1999) Multi-scale alluvial fan heterogeneity modelled with transition probability geostatistics in a sequence stratigraphic framework. J Hydrol 226(1–2):48–65

Weissmann GS, Zhang Y, LaBolle EM, Fogg GE (2002) Dispersion of groundwater age in an alluvial aquifer system. Water Resour Res 38 (10), 1198. DOI 10.1029/2001WR000907

Wen XH, Gomez Hernandez JJ (1996) Upscaling hydraulic conductivities in heterogeneous media: an overview. J Hydrol 183(1–2):9–32

Wen XH, Durlofsky LJ, Edwards MG (2003) Use of border regions for improved permeability upscaling. Math Geol 35:521–547

Wen XH, Chen YG, Durlofsky LJ (2006) Efficient 3D implementation of local-global upscaling for reservoir simulation. SPE J 11:443–453

Western AW, Blöschl G, Grayson RB (1998) How well do indicator variograms capture the spatial connectivity of soil moisture? Hydrol Process 12(12):1851–1868

Western AW, Blöschl G, Grayson RB (2001) Toward capturing hydrologically significant connectivity in spatial patterns. Water Resour Res 37(1):83–97

Yong Z (2004) Upscaling conductivity and porosity in three-dimensional heterogeneous porous media. Chin Sci Bull 49 (22):2415–2423

Zappa G, Bersezio R, Felletti F, Giudici M (2006) Modeling heterogeneity of gravel-sand, braided stream, alluvial aquifers at the facies scale. J Hydrol 325(1–4):134–153

Zhang Y, Gable CW, Person M (2006) Equivalent hydraulic conductivity of an experimental stratigraphy: implications for basin-scale flow simulations. Water Resour Res 42(5), W05404. DOI 10.1029/2005WR004720

Zhang Y, Person M, Gable CW (2007) Representative hydraulic conductivity of hydrogeologic units: insights from an experimental stratigraphy. J Hydrol 339:65–78

Zinn B, Harvey CF (2003) When good statistical models of aquifer heterogeneity go bad: a comparison of flow, dispersion, and mass transfer in connected and multivariate Gaussian hydraulic conductivity fields. Water Resour Res 39(3), 1051.